




RESEARCH PAPER

# Ammonium and nitrate regulate $\text{NH}_4^+$ uptake activity of Arabidopsis ammonium transporter AtAMT1;3 via phosphorylation at multiple C-terminal sites

Xiangyu Wu<sup>1</sup>, Ting Liu<sup>1,2</sup>, Yongjian Zhang<sup>1</sup>, Fengying Duan<sup>1</sup>, Benjamin Neuhäuser<sup>3</sup>, Uwe Ludwig<sup>3</sup>, Waltraud X. Schulze<sup>4</sup> and Lixing Yuan<sup>1,\*</sup> 

<sup>1</sup> Key Lab of Plant-Soil Interaction, MOE, College Resources and Environmental Sciences, China Agricultural University, 100193 Beijing, China

<sup>2</sup> College of Life Sciences, Hebei Normal University, 050024 Shijiazhuang, Hebei, China

<sup>3</sup> Institute of Crop Science, Nutritional Crop Physiology, University of Hohenheim, D-70593 Stuttgart, Germany

<sup>4</sup> Institute for Physiology and Biotechnology of Plants, Plant Systems Biology, University of Hohenheim, Garbenstraße 30, 70593 Stuttgart, Germany

\* Correspondence: [yuanlixing@cau.edu.cn](mailto:yuanlixing@cau.edu.cn)

Received 24 February 2019; Editorial decision 1 May 2019; Accepted 4 May 2019

Editor: Hideki Takahashi, Michigan State University, USA

## Abstract

**In plants, nutrient transporters require tight regulation to ensure optimal uptake in complex environments. The activities of many nutrient transporters are post-translationally regulated by reversible phosphorylation, allowing rapid adaptation to variable environmental conditions. Here, we show that the Arabidopsis root epidermis-expressed ammonium transporter AtAMT1;3 was dynamically (de-)phosphorylated at multiple sites in the cytosolic C-terminal region (CTR) responding to ammonium and nitrate signals. Under ammonium resupply rapid phosphorylation of a Thr residue (T464) in the conserved part of the CTR (CTR<sup>C</sup>) effectively inhibited AtAMT1;3-dependent  $\text{NH}_4^+$  uptake. Moreover, phosphorylation of Thr (T494), one of three phosphorylation sites in the non-conserved part of the CTR (CTR<sup>NC</sup>), moderately decreased the  $\text{NH}_4^+$  transport activity of AtAMT1;3, as deduced from functional analysis of phospho-mimic mutants in yeast, oocytes, and transgenic Arabidopsis. Double phospho-mutants indicated a role of T494 in fine-tuning the  $\text{NH}_4^+$  transport activity when T464 was non-phosphorylated. Transient dephosphorylation of T494 with nitrate resupply closely paralleled a transient increase in ammonium uptake. These results suggest that T464 phosphorylation at the CTR<sup>C</sup> acts as a prime switch to prevent excess ammonium influx, while T494 phosphorylation at the CTR<sup>NC</sup> fine tunes ammonium uptake in response to nitrate. This provides a sophisticated regulatory mechanism for plant ammonium transporters to achieve optimal ammonium uptake in response to various nitrogen forms.**

**Keywords:** Ammonium transporter (AMT), ammonium uptake, membrane transport, multisite phosphorylation, nitrogen signals, phosphorylation, post-translational regulation.

---

Abbreviations: ACTPK1, ACT domain protein kinase 1; AHA2, P-type  $\text{H}^+$ -ATPase 2; AMT, ammonium transporter; AMT1, AMT1-type ammonium transporter; CBL1, calcineurin B-like protein 1; CIPK23, calcineurin B-like protein-interacting protein kinase 23; CTR, C-terminal region; CTR<sup>C</sup>, conserved part of the CTR; CTR<sup>NC</sup>, non-conserved part of the CTR; qPCR, quantitative RT-PCR; STY, serine/threonine/tyrosine; Thr<sup>CTR</sup>, the conserved Thr residue in the CTR.

© The Author(s) 2019. Published by Oxford University Press on behalf of the Society for Experimental Biology.

This is an Open Access article distributed under the terms of the Creative Commons Attribution Non-Commercial License (<http://creativecommons.org/licenses/by-nc/4.0/>), which permits non-commercial re-use, distribution, and reproduction in any medium, provided the original work is properly cited. For commercial re-use, please contact [journals.permissions@oup.com](mailto:journals.permissions@oup.com)

## Introduction

Ammonium is a major nitrogen (N) form in most soils and is preferentially taken up, providing an essential N metabolite in plants (Marschner and Rengel, 2012). Ammonium may also act as a nutrient signal molecule to trigger physiological and morphological responses in plants (Lima *et al.*, 2010; Liu and von Wirén, 2017). High-affinity ammonium uptake and root-to-shoot ammonium translocation are mainly mediated by ammonium transporters (AMTs), which belong to the AMT/MEP/Rh protein superfamily (Loqué and von Wirén, 2004). In Arabidopsis roots, the epidermis-expressed AtAMT1;1 and AtAMT1;3 and the endodermis-expressed AtAMT1;2 control uptake of ammonium via the symplastic and apoplastic transport pathway, respectively (Kaiser *et al.*, 2002; Loqué *et al.*, 2006; Mayer *et al.*, 2006; Mayer and Ludewig 2006; Neuhäuser *et al.*, 2007; Yuan *et al.*, 2007a; Duan *et al.*, 2018). AtAMT2;1 shows marginal expression in the epidermis, but is preferentially localized to the pericycle cells under elevated ammonium supply and is involved in the root-to-shoot translocation of ammonium (Neuhäuser *et al.*, 2009; Giehl *et al.*, 2017).

To respond to external N availability and the internal plant N status, AMT gene expression is tightly controlled in roots at multiple regulatory levels. At the transcriptional level, ammonium supply can either up- or down-regulate expression of AMTs, which is probably triggered by a downstream metabolite of ammonium, i.e. glutamine (Gazzarrini *et al.*, 1999; Rawat *et al.*, 1999; von Wirén *et al.*, 2000; Sonoda *et al.*, 2003a,b; Gu *et al.*, 2013; Wu *et al.*, 2015). The transcription factors of nitrate-inducible GARP-type transcriptional repressor 1 (NIGT1)/hypersensitive to low P<sub>i</sub>-elicited primary root shortening 1 (HRS1) negatively regulate expression of *AtAMT1;1*, while the rice transcription factors growth regulation factor 4 (GRF4) and indeterminate domain 10 (IDD10) activate expression of *OsAMT1;1* and *OsAMT1;2*, respectively (Xuan *et al.*, 2013; Kiba *et al.*, 2018; Li *et al.*, 2018). At the post-transcriptional level, *AtAMT1;1* mRNA turnover is strictly controlled by plant N availability (Yuan *et al.*, 2007b).

To cope with elevated external ammonium, Arabidopsis AMT1-type ammonium transporters (AtAMT1s) can be post-translationally modified via phosphorylation of their cytosolic C-terminal region (CTR) to shut off their transport activity (Loqué *et al.*, 2007; Neuhäuser *et al.*, 2007; Lanquar *et al.*, 2009; Yuan *et al.*, 2013). Within the homo- or hetero-trimeric complexes of AMT1s, the CTR interacts with a cytosolic loop of its own or the adjacent monomer (Khademi *et al.*, 2004; van den Berg *et al.*, 2016). The phosphorylation of a conserved Thr residue in the CTR (Thr<sup>CTR</sup>) can lead to *trans*-inactivation of the whole complex in an allosteric manner (Loqué *et al.*, 2007; Neuhäuser *et al.*, 2007; Yuan *et al.*, 2013). The Thr<sup>CTR</sup> of AtAMT1;1 (T460) and AtAMT1;2 (T472) are phosphorylated by the calcineurin B-like protein-interacting protein kinase 23 (CIPK23)-calcineurin B-like protein 1 (CBL1) complex, while OsAMT1;2 (T453) is phosphorylated by the serine/threonine/tyrosine (STY) kinase ACT domain protein kinase 1 (ACTPK1) (Straub *et al.*, 2017; Beier *et al.*, 2018). In both cases, phosphorylation is triggered by an ammonium signal. Phosphorylation of Thr<sup>CTR</sup> in AtAMT1;3 (T464) has also been

detected *in vivo* by phosphoproteomics and is able to regulate the transporter activity (Yuan *et al.*, 2013; Menz *et al.*, 2016). However, AtAMT1;3 T464 is not the target of AtCIPK23-CBL1, even though its conserved phosphorylation target site is indistinguishable from those of other AtAMT1s by sequence (Straub *et al.*, 2017). Besides Thr<sup>CTR</sup>, other phosphorylation sites in the CTRs of AtAMT1;1 and AtAMT1;3 have been identified by previous phosphoproteomic studies *in vivo* (Lanquar *et al.*, 2009; Engelsberger and Schulze, 2012; Menz *et al.*, 2016). Notably, distinct dynamic phosphorylation patterns on these multiple sites were observed in plants in response to changes in the N nutritional status, including supplies of different forms of N. Whether these multiple phosphorylation sites are functionally involved in regulating AMT1s transporter activity and how they differentially respond to variable N supply, however, remain to be elucidated.

Here, we assessed the correlations between <sup>15</sup>N-labeled high-affinity ammonium influx and multisite phosphorylation status of AtAMT1;3 CTR in Arabidopsis roots, and showed that ammonium resupply-triggered phosphorylation of T464 in the conserved part of the CTR rapidly decreased ammonium uptake. However, nitrate resupply led to a transient dephosphorylation of T494 in the non-conserved part of the CTR, accompanied by an increase in ammonium uptake. Using yeast, oocytes, and transgenic Arabidopsis, AtAMT1;3 T464, T494 single or double phospho-mimic variants generated by site-directed mutagenesis were functionally analysed *in vitro* and *in vivo*. The results indicated that T494 phosphorylation could partially decrease AtAMT1;3 transporter activity and this fine-tuning role of T494 relied on the non-phosphorylation status of T464. These findings thus extend our understanding of AtAMT1s phospho-dependent regulation from single to multiple site levels, and highlight the mechanisms by which these multisite phosphorylation/dephosphorylation processes cooperate to achieve optimal uptake of ammonium under control of different N signals.

## Materials and methods

### Vector constructs

The open reading frame of *AtAMT1;3* (*AtAMT1;3-ORF*) was cloned into vector pTOPO (Invitrogen) and sub-cloned into yeast expression vector p426-HXT7 through the *EcoRI* site, yielding the plasmid p426-*AtAMT1;3*. Mutations were introduced into *AtAMT1;3-ORF* by using the Q5® Site-Directed Mutagenesis Kit (NEB) with specific primers (Supplementary Table S1 at JXB online) and verified by sequencing, yielding the plasmids p426-*AtAMT1;3* T464A, p426-*AtAMT1;3* T464D, p426-*AtAMT1;3* H474stop, p426-*AtAMT1;3* S480A, p426-*AtAMT1;3* S480D, p426-*AtAMT1;3* S487A, p426-*AtAMT1;3* S487D, p426-*AtAMT1;3* T494A, p426-*AtAMT1;3* T494D, p426-*AtAMT1;3* T464A T494A, p426-*AtAMT1;3* T464A T494D, p426-*AtAMT1;3* T464D T494A, p426-*AtAMT1;3* T464D T494D, p426-*AtAMT1;3* T464A S480A S487A, and p426-*AtAMT1;3* T464A S480D S487D for yeast transformation.

The *AtAMT1;3* promoter (*AtAMT1;3pro*) was amplified by PCR from the pBI101-*AtAMT1;3pro::AtAMT1;3::GFP* construct (Loqué *et al.*, 2006) using the specific primers *AtAMT1;3pro-XbaI* and *AtAMT1;3pro-ApaI* (Supplementary Table S1). The amplified fragment was digested by *XbaI* and *ApaI*, and cloned into vector pT-Hygro mycin

to generate the pT-*AtAMT1;3pro* construct. The *AtAMT1;3-ORF* and *AtAMT1;3* phospho-mutants were amplified by PCR using specific primers (Supplementary Table S1) and cloned into the pT-*AtAMT1;3pro* construct through the *Apal* site, resulting in the plasmids pT-*AtAMT1;3pro::AtAMT1;3*, pT-*AtAMT1;3pro::AtAMT1;3 T464A*, pT-*AtAMT1;3pro::AtAMT1;3 T494A*, pT-*AtAMT1;3pro::AtAMT1;3 T494D*, pT-*AtAMT1;3pro::AtAMT1;3 T464A T494A*, and pT-*AtAMT1;3pro::AtAMT1;3 T464A T494D* for Arabidopsis transformation.

The *AtAMT1;3-ORF* and *AtAMT1;3* phospho-mutants were amplified by PCR with specific primers (Supplementary Table S1) and cloned into the oocyte expression vector pOO2 through *SpeI* and *EcoRI* sites (Baukowitz *et al.*, 1999), yielding the plasmids pOO2-*AtAMT1;3*, pOO2-*AtAMT1;3 T494A*, pOO2-*AtAMT1;3 T494D*, pOO2-*AtAMT1;3 T464A*, pOO2-*AtAMT1;3 T464A T494A*, and pOO2-*AtAMT1;3 T464A T494D* for oocyte assays.

#### Growth complementation and <sup>15</sup>N-labeled ammonium uptake assays in yeast

The plasmids were heated shock-transformed in triple-*Δmep* (1–3) deletion yeast strain 31019b (Marini *et al.* 1997), and the transformants were selected on solid YNB medium with arginine (Arg) (2% Agar, YNB without amino acids and ammonium sulfate (Difco), 3% glucose and 0.1% Arg). A growth complementation assay was performed on solid YNB medium supplemented with 3% glucose, 1 mM NH<sub>4</sub>Cl or 1 mM Arg as the sole nitrogen source, buffered with 50 mM MES/Tris (pH 5.5). The <sup>15</sup>N-labeled ammonium uptake assay was performed at a concentration of 250 μM <sup>15</sup>NH<sub>4</sub><sup>+</sup> (99.12 atom% <sup>15</sup>N) as described previously by Loqué *et al.* (2009).

#### Electrophysiological measurements, preparation and injection of oocytes

The electrophysiological methods used were described by Mayer and Ludewig (2006). The oocytes were from Ecocyte Bioscience (Castrop-Rauxel), presorted again and injected with 50 nl of cRNA (1 μg μl<sup>-1</sup>). Oocytes were kept in ND96 for 4 d at 18 °C and then placed in a small recording chamber. The recording solution was 110 mM choline chloride, 2 mM CaCl<sub>2</sub>, 2 mM MgCl<sub>2</sub>, and 5 mM MES, pH adjusted to 5.5 with Tris. Variable ammonium concentrations were added as NH<sub>4</sub>Cl salt. Currents without added ammonium were subtracted at each voltage.

#### Generation of transgenic Arabidopsis plants

Arabidopsis mutant *qko* (*atamt1;1*, *atamt1;2*, *atamt1;3* and *atamt2;1*) was used for transformation (Yuan *et al.*, 2007a). *Agrobacterium*-mediated transformation was performed using *Agrobacterium tumefaciens* strain GV3101 by the standard floral-dip method (Clough and Bent, 1998). Transgenic lines were selected on half-strength Murashige & Skoog medium containing 25 mg l<sup>-1</sup> hygromycin B. Independent T3 homozygotes with a single-copy transgene were used for the analysis. Plants were grown in a climate-controlled greenhouse under 16/8 h light/dark cycle at temperature 22 °C/18 °C.

#### <sup>15</sup>N-labeled ammonium influx assay in roots

Arabidopsis plants were cultured hydroponically as described by Loqué *et al.* (2006). Six-week-old Arabidopsis plants were grown hydroponically in a growth cabinet at 22 °C with 10 h light/14 h dark photoperiod illuminated at 100 μmol m<sup>-2</sup> s<sup>-1</sup>. After 4 d N starvation, 4 mM NH<sub>4</sub>Cl or 4 mM KNO<sub>3</sub> was used for ammonium or nitrate resupply treatment, respectively. All nutrient solutions were adjusted to pH 5.8. Nutrient solutions were renewed every other day. Influx of <sup>15</sup>N-labeled NH<sub>4</sub><sup>+</sup> into roots of Arabidopsis plants was measured after rinsing the roots of hydroponically grown plants in 1 mM CaSO<sub>4</sub> solution for 1 min, followed by an incubation for 6 min in full nutrient solution (pH 5.8) containing 250 μM concentrations of <sup>15</sup>N-labeled NH<sub>4</sub><sup>+</sup> (99.12 atom% <sup>15</sup>N) as the

sole N source, and a final wash in 1 mM CaSO<sub>4</sub> solution for 1 min. Then roots were harvested and freeze-dried at -50 °C. A 1 mg aliquot of ground samples was used for <sup>15</sup>N determination by isotope mass spectrometry (DELTAplus XP, Thermo-Finnigan).

#### RNA extraction and quantitative RT-PCR analysis

Total RNA was extracted from roots of hydroponic grown plants using RNAiso Plus (Takara). RNA samples were pretreated with gDNA Eraser of the PrimeScript™ RT reagent Kit (Takara) and reverse transcribed into cDNA. Using the IQ5 Real-Time PCR System (Bio-Rad), quantitative RT-PCR (qPCR) was performed with SYBR Green. Expression of *AtUBQ10* and *AtEIF4a* (Boudsocq *et al.*, 2010) was used for normalizing gene expression. The specific primers used in the qPCR analysis are listed in Supplementary Table S1.

#### Protein gel blot analysis

The microsomal membrane fraction was isolated from Arabidopsis roots as described by Yuan *et al.* (2007a). AtAMT1;3 polyclonal antibodies were produced against peptide sequences at the C-terminus (n-DPGSPFPRSATPPRV-c) (Beijing Protein Innovation Co., Ltd); the AtAMT1s T<sup>CTR</sup> phosphorylation specific antibody (AtAMT1s T<sup>CTR</sup>-P) was described by Straub *et al.* (2017). Protein (15 μg) was denatured with loading buffer at 37 °C for 30 min, separated on 10% SDS polyacrylamide gels, and transferred to a polyvinylidene difluoride (PVDF) membrane (Amersham Hybond-P; 0.45 μm; GE Healthcare) by electroblotting. Protein was stained with Coomassie Brilliant Blue as the loading control. The PVDF membrane was blocked by incubation in PBST with 5% skim milk powder for 1 h at room temperature and incubated with primary antibodies (1:5000 for anti-AtAMT1;3 and 1:500 for anti-AtAMT1s T<sup>CTR</sup>-P) and secondary antibodies (1:10 000) followed by ECL detection (Amersham ECL™ Advance Western Blotting Detection Kit). MagicMark™ XP Western Standard (Invitrogen) and Blue Plus IV Protein Marker (TransGen Biotech) were used to indicate the molecular masses of proteins.

## Results

### *AtAMT1;3*-dependent ammonium uptake in Arabidopsis roots was rapidly repressed by resupply of ammonium, but transiently induced by nitrate

To investigate whether AtAMT1;3 transporter activity in roots differentially responds to resupply of ammonium or nitrate, we employed the Arabidopsis mutant *qko+13* in which *AtAMT1;3* expression was reconstituted in the *amt-qko* background (*atamt1;1*, *atamt1;2*, *atamt1;3*, *atamt2;1*), allowing us to quantify AtAMT1;3-dependent ammonium uptake capacity due to the disruption of three other endogenous *AtAMT* genes (Yuan *et al.*, 2007a). Hydroponically grown *qko+13* seedlings were starved of N, and resupplied with 4 mM ammonium or nitrate for different time periods. With these plants, a short-term high-affinity <sup>15</sup>N-labeled ammonium influx assay was performed in roots. *AtAMT1;3* expression was simultaneously quantified at the transcript level by qPCR and at the protein level by western blot analysis (Fig. 1). Ammonium influx rates in roots of *qko+13* were rapidly decreased up to approx. 30% within 15 min of ammonium resupply compared with that under N deficiency (Fig. 1A). With resupply of nitrate, however, ammonium influx rates were transiently induced up to 17% within 15 min and then returned to the original level after 30 min. Compared with that in N-deficient



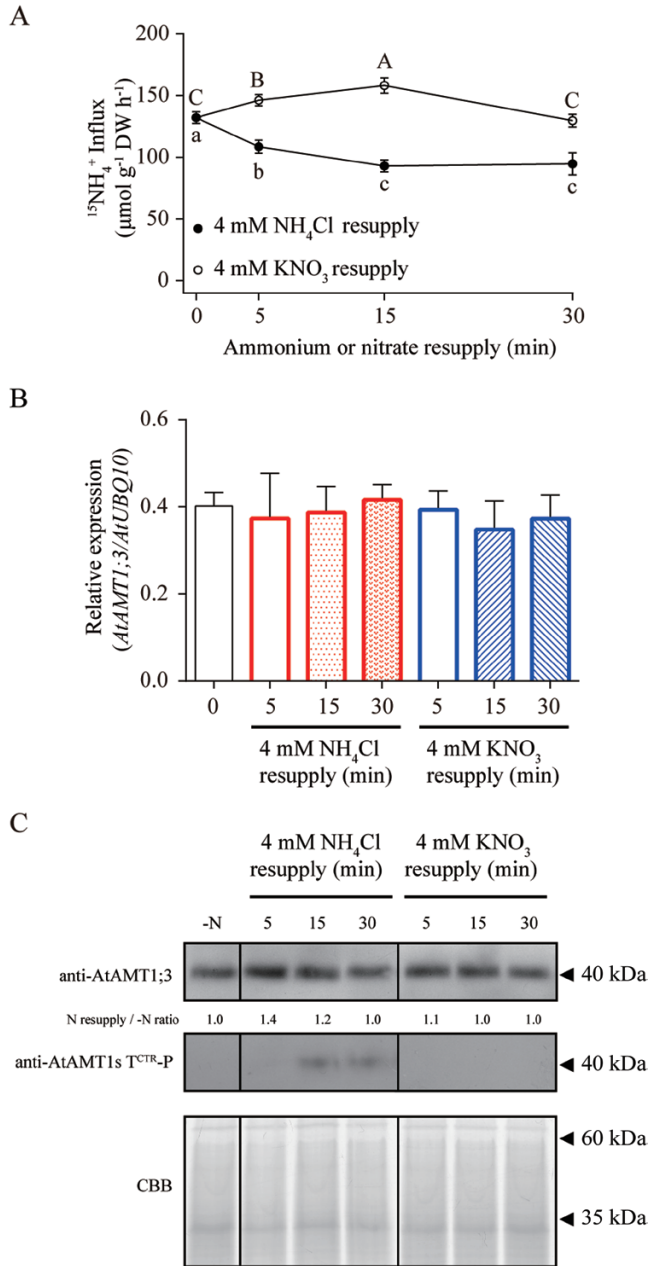


**Fig. 1.** Dynamic patterns of AtAMT1;3-dependent root ammonium uptake and T464 phosphorylation in response to ammonium and nitrate resupply. Six-week-old hydroponically grown Arabidopsis mutant *qko+13* (*atamt1;1*, *atamt1;2* and *atamt2;1*) were subjected to N starvation for 4 d, and then resupplied with 4 mM  $\text{NH}_4\text{Cl}$  or 4 mM  $\text{KNO}_3$  for 5, 15, and 30 min. (A)  $^{15}\text{N}$ -labeled ammonium influx in roots determined at the concentration of 250  $\mu\text{M}$ . (B) Transcript expression levels of *AtAMT1;3* in roots quantified by qPCR with three replicates, and normalized by *AtUBQ10* expression level. (C) Protein expression levels of AtAMT1;3 and phosphorylated AtAMT1;3 at T464 in roots determined by western blot analysis using anti-AtAMT1;3 and anti-AMT1s  $\text{Thr}^{\text{CTR}}\text{-P}$  antibody, respectively, normalized by Coomassie Brilliant Blue staining. Bars indicate means  $\pm$ SD ( $n=3$ ) and significant differences at  $P<0.001$  according to Tukey's test are indicated by different letters. (This figure is available in color at JXB online.)

roots, the abundance of *AtAMT1;3* transcripts did not show any change after resupply of ammonium or nitrate (Fig. 1B; Supplementary Fig. S1). Similarly, no change was observed at the protein levels as revealed by western blot analysis using an AtAMT1;3-specific antibody (Fig. 1C). Thus, these results

revealed distinct dynamic patterns for AtAMT1;3 activity changes in response to different N forms. This regulation was at the post-translational level, because the transcript and protein abundances of AtAMT1;3 did not change accordingly.

*Ammonium signals triggered AtAMT1;3 phosphorylation at T464 in the  $\text{CTR}^{\text{C}}$ , whereas nitrate signals triggered multisite (de-)phosphorylation in the  $\text{CTR}^{\text{NC}}$*

Alignment of AtAMT1s amino acids sequences showed that their CTR consisted of a conserved ( $\text{CTR}^{\text{C}}$ ) and a non-conserved ( $\text{CTR}^{\text{NC}}$ ) part, which is a common feature for AMT/MEP family members (Fig. 2A; Loqué *et al.*, 2007). By collecting the phosphorylated peptide sequences available from previous phosphoproteomics or phospho-specific antibody analyses of different Arabidopsis organs under various treatments, the number of *in vivo* phosphorylated Ser/Thr residues identified in the CTR was eight for AtAMT1;1, one for AtAMT1;2, and four for AtAMT1;3 (Supplementary Table S2). In the  $\text{CTR}^{\text{C}}$ , only a single conserved phosphorylated residue ( $\text{Thr}^{\text{CTR}}$ ) appeared (AtAMT1;1 T460/AtAMT1;2 T472/AtAMT1;3 T464) (Fig. 2A). In the  $\text{CTR}^{\text{NC}}$ , however, multiple phosphorylation sites were present in AtAMT1;1 (seven residues) and AtAMT1;3 (three residues), particularly two conserved Ser (AtAMT1;1 S475/AtAMT1;3 S480, AtAMT1;1 S488/AtAMT1;3 S487) and one conserved Thr (AtAMT1;1 T497/AtAMT1;3 T494). Apart from the well-characterized  $\text{Thr}^{\text{CTR}}$ , multiple phosphorylation sites resided in the  $\text{CTR}^{\text{NC}}$ , but potential functional roles in regulating ammonium transporters are unknown.

To test whether resupply of ammonium can trigger AtAMT1;3 T464 phosphorylation in the  $\text{CTR}^{\text{C}}$  and thereby inhibit ammonium uptake capacity in *qko+13* roots, a phospho-specific antibody against  $\text{Thr}^{\text{CTR}}$  of AtAMT1s (Straub *et al.*, 2017) was employed for western blot analysis (Fig. 1C). Due to an exclusive expression of AtAMT1;3 in *qko+13* roots, the band detected by this antibody reflects phosphorylation of AtAMT1;3 at T464. Compared with N-deficient roots, the phosphorylated polypeptides appeared after 15 min resupply of ammonium (Fig. 1C) and coincided with decreases of AtAMT1;3-dependent ammonium uptake capacity (Fig. 1A). No T464 phosphorylation, however, was detected under nitrate resupply. Because T464 phosphorylation inactivates AtAMT1;3 transporter activity (Yuan *et al.*, 2013), this result suggested that ammonium signals, but not nitrate, selectively induced T464 phosphorylation and thereby inhibited root ammonium uptake capacity.

With resupply of nitrate, but not ammonium, considerable phosphorylated Ser/Thr residues in the  $\text{CTR}^{\text{NC}}$  of AtAMT1;3 were identified by previous phosphoproteomics of Arabidopsis plants (Engelsberger and Schulze, 2012; Fig. 2B; Supplementary Fig. S2). Among them, two Ser residues (S480/S487) were simultaneously phosphorylated, and the phosphorylation levels were increased up to 2-fold after 3 min resupply of nitrate to N-deficient seedlings. The phosphorylated Thr residue (T494), by contrast, was rapidly dephosphorylated within 5 min under nitrate resupply, and then returned to the original level after

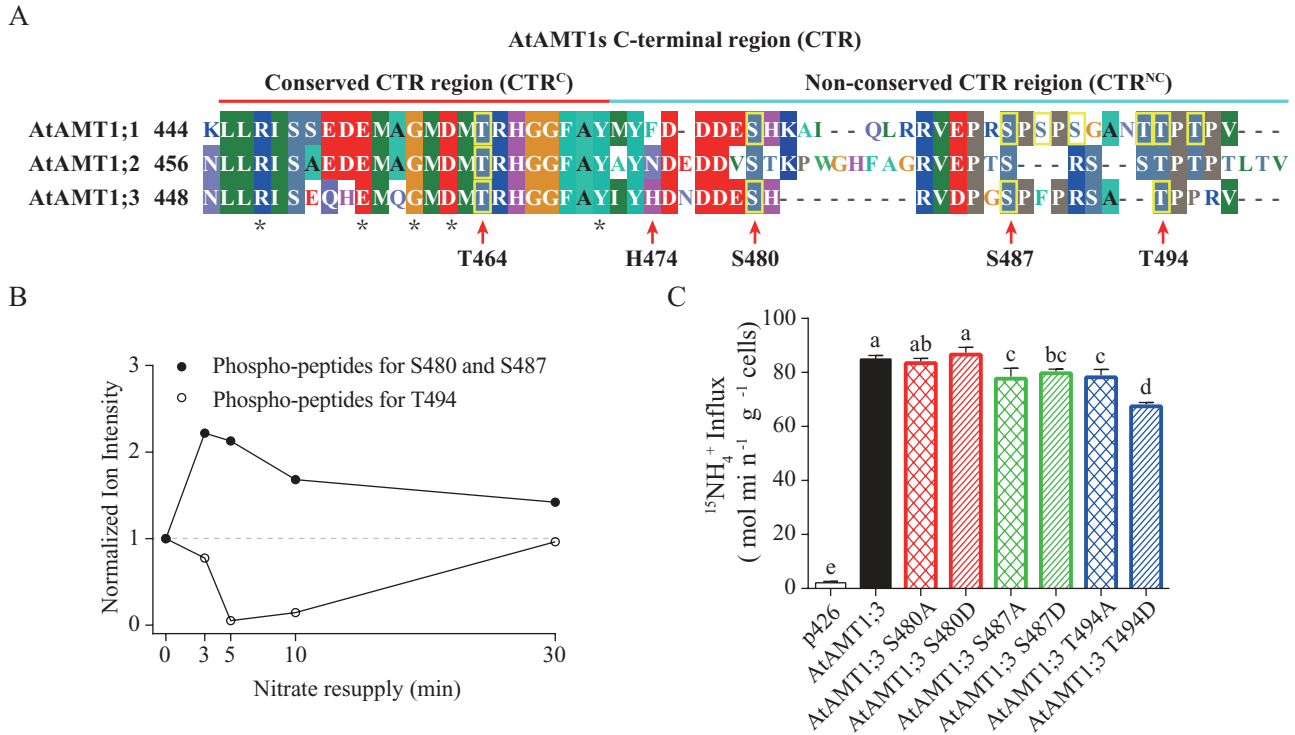


**Fig. 2.** Phosphorylation dynamics of AtAMT1;3 CTR<sup>NC</sup> at multiple sites (S480, S487, and T494) in response to nitrate and functional analysis of corresponding phospho-mutants in yeast. (A) *In vivo* phosphorylation sites in the CTR of AtAMT1s identified by phosphoproteomics and phospho-specific antibodies (Supplementary Table S1). Alignment of amino acid sequences showed that the CTR of AtAMT1s consisted of a conserved (CTR<sup>C</sup>) and a non-conserved (CTR<sup>NC</sup>) part that are underlined in red and blue, respectively. The phosphorylated Thr/Ser residues are labeled with a yellow box. Five universally conserved residues within the CTR<sup>C</sup>, including the 'ExxGxD' motif, are labeled with asterisks. (B) Normalized ion intensity of phosphorylated AtAMT1;3 peptides HGGFAYIYHDNDDES(ph)HRVDPGS(ph)PFPR (S480/S487) and SAT(ph)PPRV (T494) that responded to nitrate. The data were obtained from Engelsberger and Schulze (2012). (C) Influx of <sup>15</sup>N-labeled ammonium into yeast mutant 31019b expressing empty vector p426, AtAMT1;3 wild type, and different AtAMT1;3 phospho-variants: S480A, S480D, S487A, S487D, T494A, and T494D. Influx assays were performed at the concentration of 250  $\mu$ M. Bars indicate means  $\pm$ SD ( $n=5$ ) and significant differences at  $P<0.001$  according to Tukey's test are indicated by different letters.

30 min. Thus, a close correlation between dynamic changes of S480/S487/T494 phosphorylation status and ammonium uptake rates in roots of *qko+13* (Fig. 1A) may suggest that nitrate signals could control multisite phosphorylation/dephosphorylation in the CTR<sup>NC</sup> for regulating AtAMT1;3 transporter activity.

#### T494 phosphorylation in the CTR<sup>NC</sup> was involved in regulating AtAMT1;3 transporter activity *in vitro* and *in vivo*

To verify whether phosphorylation sites in the CTR<sup>NC</sup> are involved in regulating AtAMT1;3 transporter activity, mutants mimicking non-phosphorylation (Ser/Thr replaced by Ala) and phosphorylation (Ser/Thr replaced by Asp) of each site were generated (Fig. 2C). These AtAMT1;3 phospho-variants together with the wild type were then functionally analysed in the yeast strain 31019b (triple-*mepΔ*), which grows poorly on <5 mM ammonium as a sole N source (Marini *et al.*, 1997). The yeast cells expressing all variants were able to confer growth complementation on 1 mM ammonium, and no visible growth difference was observed between the wild type and phospho-mutants (Supplementary Fig. S3). By quantitative analysis using a short-term <sup>15</sup>NH<sub>4</sub><sup>+</sup> uptake assay, it was found

that the mutations at S487 and T494, but not S480, resulted in significant decreases of transporter activity compared with that of the wild type (Fig. 2C). The S487 phospho-mutants showed approx. 8% reduction, but no difference was observed between the non-phosphorylated (S487A) and phosphorylated form (S487D). However, compared with the non-phosphorylation mimic T494A, the phosphorylated mimic T494D revealed a significantly lower transporter activity (~10%), suggesting that AtAMT1;3 transporter activity is modulated via the T494 phosphorylation/dephosphorylation modification. Under nitrate resupply, the T494 dephosphorylation (derepressed activity) occurred within 5 min, closely paralleling the enhanced ammonium uptake rates in roots of *qko+13* (Fig. 1A). This was followed by T494 phosphorylation (repressed activity) after 30 min, when the uptake had returned to the original level. Among these multisite phosphorylations, T494 phospho-modification was controlled by nitrate signals for regulating AtAMT1;3-dependent ammonium uptake in roots.

The AtAMT1;3 T494 phospho-mutants together with the wild type were then functionally characterized in *Xenopus* oocytes (Fig. 3). At -100 mV, oocytes expressing AtAMT1;3 T494A and T494D variants showed NH<sub>4</sub><sup>+</sup>-specific inward currents resulting from electrogenic transport of ammonium (NH<sub>4</sub><sup>+</sup>) into the oocytes. These ammonium-induced currents

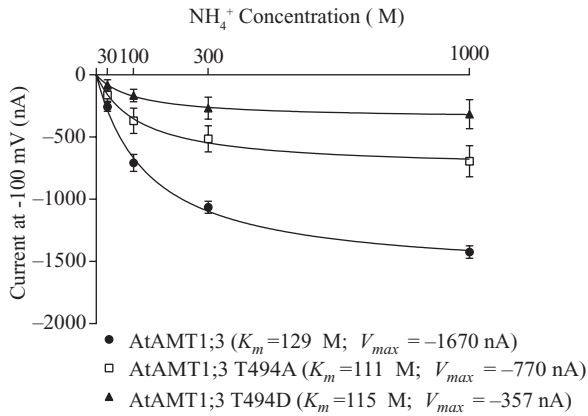


**Fig. 3.** Functional characterization of AtAMT1;3 T494 phospho-mutants in *Xenopus* oocytes. Kinetic properties of ammonium-induced currents in oocytes injected with *AtAMT1;3*, and *AtAMT1;3* phospho-mutants *T494A* and *T494D*. Inward currents were plotted under conditions of 30–1000  $\mu$ M NH<sub>4</sub>Cl at –100 mV. Bars indicate means  $\pm$ SD ( $n \geq 4$ ). From a fit with the Michaelis–Menten equation,  $V_{max}$  and  $K_m$  were calculated.

saturated in response to external ammonium concentrations that ranged from 30 to 1000  $\mu$ M. The concentration needed to achieve half-maximal current ( $K_m$ ) was similar among AtAMT1;3 (129  $\mu$ M), T494A (111  $\mu$ M) and T494D (115  $\mu$ M). However, compared with the maximal mean current ( $V_{max}$ ) of the AtAMT1;3 wild type (–1670 nA), the T494A and T494D mutants had a considerably lower  $V_{max}$  of –770 and –357 nA, respectively. Transporter activity of the phosphorylation-mimic variant (T494D) was half that of the non-phosphorylation mimic (T494A). This result suggested that T494 phosphorylation was able to down-regulate AtAMT1;3 transporter activity without affecting the substrate affinity.

To further confirm whether T494 phosphorylation can regulate AtAMT1;3-dependent ammonium uptake *in vivo*, the *AtAMT1;3* T494 phospho-variants together with the wild type were expressed in the *Arabidopsis qko* mutant background under the control of *AtAMT1;3pro* (Fig. 4). Two independent homozygous lines of each construct, *qko+AtAMT1;3pro::AtAMT1;3* (*t3* and *t17*), *qko+AtAMT1;3pro::AtAMT1;3 T494A* (*a22* and *a30*), and *qko+AtAMT1;3pro::AtAMT1;3 T494D* (*d16* and *d22*), were selected, which had similar expression levels to transgenic *AtAMT1;3* variants (Fig. 4A). The short-term <sup>15</sup>N-labeled ammonium influx assay was then performed in N-deficient roots at a concentration of 250  $\mu$ M, allowing the quantitative evaluation of transport capacity of AtAMT1;3 variants *in vivo* (Fig. 4B). The *qko* is defective in four endogenous *AtAMT* genes (*AtAMT1;1*, *AtAMT1;2*, *AtAMT1;3*, and *AtAMT2;1*) and loses up to 90% of high-affinity ammonium uptake capacity in roots (Yuan *et al.*, 2007a). Compared with *qko*, the transgenic lines expressing *AtAMT1;3 T494A* or *T494D* showed significantly enhanced ammonium influx rates. The *in vivo* transport activity of each variant was further determined after subtraction of the residual background transport activity of *qko*. Compared with the AtAMT1;3 wild type, T494A and T494D showed reduced activities of up to 18 and 33%, respectively (Fig. 4B). Similar to yeast and oocytes, the T494 phosphorylated form (T494D) of AtAMT1;3 conferred an 18% lower

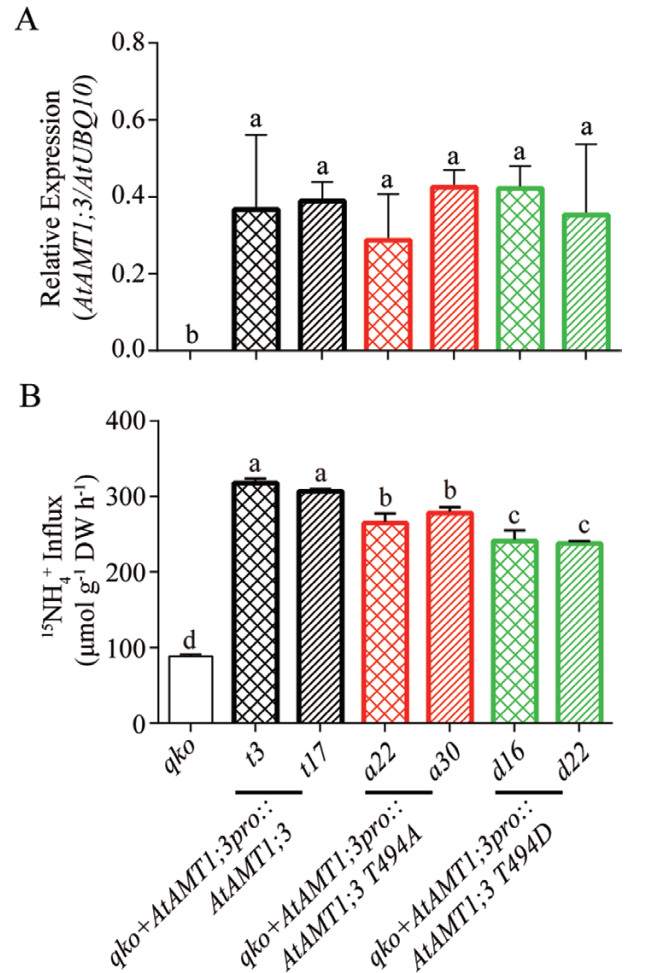


**Fig. 4.** Functional characterization of AtAMT1;3 T494 phospho-mutants in transgenic *Arabidopsis* roots. (A) Transcript expression levels of *AtAMT1;3* in roots of *qko*, *qko+AtAMT1;3pro::AtAMT1;3*, *qko+AtAMT1;3pro::AtAMT1;3 T494A* or *qko+AtAMT1;3pro::AtAMT1;3 T494D* transgenic lines. Levels were quantified by qPCR with three replicates and normalized by *AtUBQ10* expression. (B) Influx of <sup>15</sup>N-labeled ammonium into roots of the same line as in (A). N-deficient roots were employed for <sup>15</sup>N-labeled ammonium influx assays as determined at the concentration of 250  $\mu$ M. Bars indicate means  $\pm$ SD ( $n \geq 5$ ) and significant differences at  $P < 0.001$  according to Tukey's test are indicated by different letters. (This figure is available in color at JXB online.)

ammonium uptake rate than that of the non-phosphorylation mimic T494A. These results suggest that *in vivo* phospho-dependent modification of AtAMT1;3 at T494 could moderately regulate ammonium influx rates in roots.

#### Non-phosphorylation of T464 in the CTR<sup>C</sup> was a prerequisite of fine-tuning AtAMT1;3 transport activity via T494 (de-)phosphorylation in the CTR<sup>NC</sup>

Given that phosphorylation of T464 in the CTR<sup>C</sup> and T494 in the CTR<sup>NC</sup> could negatively regulate the transport activity of AtAMT1;3 to varying extents, the possible interaction between these two phospho-dependent modifications was investigated using the corresponding double phospho-mutants (Fig. 5). As in a previous study (Yuan *et al.*, 2013), yeast cells expressing the non-phosphorylation mimic variant T464A, but not the



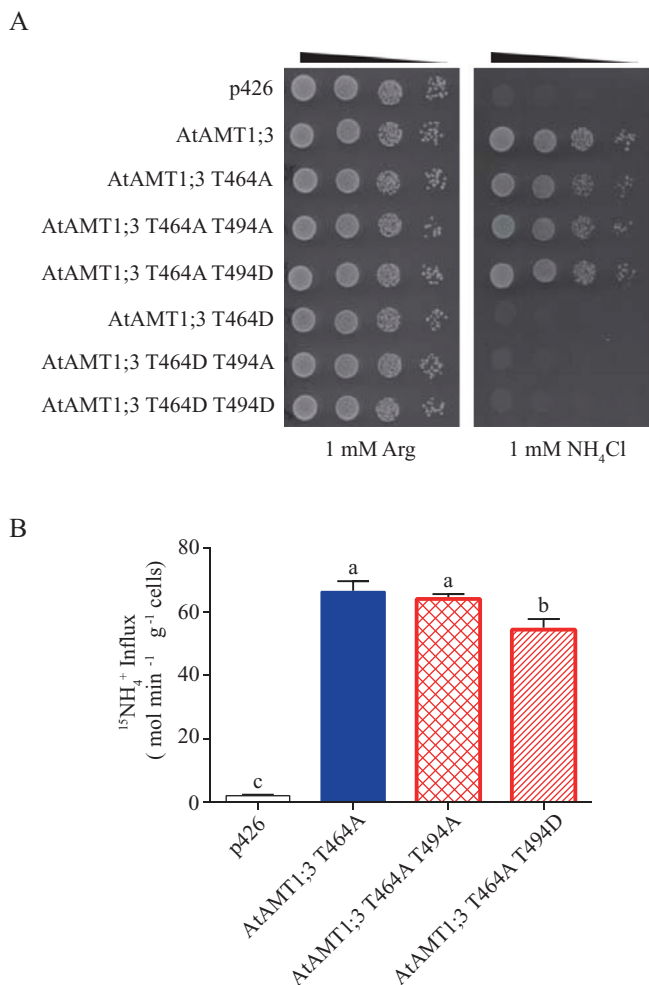


**Fig. 5.** Functional characterization of AtAMT1;3 T464 T494 double phospho-mutants in yeast. (A) Growth complementation of the yeast mutant 31019b ( $\Delta mep1-3$ ) expressing empty vector p426, AtAMT1;3 wild type, AtAMT1;3 single phospho-variant T464A or T464D, double phospho-variants T464A T494A, T464A T494D, T464D T494A, or T464D T494D. Yeast cells were spotted on YNB medium supplemented with either 1 mM Arg or 1 mM ammonium as the sole N source at pH5.5 for 3 d at 28 °C. (B) Influx of <sup>15</sup>N-labeled ammonium into yeast mutant 31019b expressing empty vector p426, AtAMT1;3 wild type, AtAMT1;3 single phospho-variant T464A and double phospho-variants T464A T494A or T464A T494D. Influx assays were performed at the concentration of 250  $\mu$ M. Bars indicate means  $\pm$ SD ( $n=5$ ) and significant differences at  $P<0.001$  according to Tukey's test are indicated by different letters. (This figure is available in color at JXB online.)

phosphorylation mimic variant T464D, were able to mediate growth under 1 mM ammonium (Fig. 5A). In the T464D background, neither phosphorylation mimic (T464D T494D) nor non-phosphorylation mimic (T464D T494A) double mutants conferred growth, resembling the single mutant T464D. In the T464A background, although all double mutants conferred yeast growth under low ammonium, the <sup>15</sup>NH<sub>4</sub><sup>+</sup> uptake assay showed that the T464A T494A double mutant had a similar activity to the single mutant T464A, while the T464A T494D double mutant revealed approx. 27% reduction of transporter activity (Fig. 5B). When expressed in oocytes, the single non-phospho-mutant T464A of AtAMT1;3 revealed unexpectedly low activity (Supplementary Fig. S4), similar

to the non-phospho-mutant of AtAMT1;2 at the equivalent site (T472A) (Neuhäuser *et al.*, 2007). Nevertheless, by adding non-phosphorylation mimic T494 to the T464A mutant in the double phospho-variant T464A T494A, the transporter activity was restored. This indicated that, in the presence of non-phosphorylated T464, T494 dephosphorylation enhanced AtAMT1;3 transporter activity. Dephosphorylation/phosphorylation modifications of AtAMT1;3 at T464 apparently turned on/off transport activity, while those modifications at T494 moderately fine-tuned transporter activity as long as T464 was not phosphorylated.

We then quantified the tuning ability of T494-dependent phosphorylation/dephosphorylation for root ammonium uptake when T464 was maintained in the non-phosphorylated status (Fig. 6). The transgenic lines *qko+AtAMT1;3pro::AtAMT1;3 T464A* (*ta14* and *ta49*), *qko+AtAMT1;3pro::AtAMT1;3 T464A T494A* (*Aa711* and *Aa402*) and *qko+AtAMT1;3pro::AtAMT1;3 T464A T494D* (*Ad1715* and *Ad2211*) were generated with similar expression levels of AtAMT1;3 variants in roots (Fig. 6A). Quantification of the <sup>15</sup>NH<sub>4</sub><sup>+</sup> influx rates in transgenic Arabidopsis roots expressing the double phospho-variant T464A T494A showed similar rates to those expressing the single phospho-variant T464A (Fig. 6B). By contrast, the lines expressing T464A T494D had approx. 32~34% reduced ammonium uptake activity compared with that of the non-phospho-mimic form T464A T494A. Thus, in addition to T464-mediated activation/inactivation, phospho-dependent modification of T494 adjusted ~30% of AtAMT1;3 transport activity in roots.

## Discussion

Phosphorylation and dephosphorylation are flexible mechanisms for regulating the function of many nutrient transporters (including AKT1, NRT1;1, PHT1;1, and AMT1s) by reversibly altering their biochemical properties, subcellular location, or protein-protein interactions (Xu *et al.*, 2006; Ho *et al.*, 2009; Bayle *et al.*, 2011; Straub *et al.*, 2017). In many cases these transporters contain multiple phosphorylation sites, which probably provide a simple means for putting two or more such effects in the same protein for greatly increased regulatory potential (Cohen, 2000; Haruta *et al.*, 2015). However, key questions remain to be addressed, including which sites are phospho-regulated under which biological conditions, as well as whether multisite phosphorylation events function independently or cooperatively to modulate transporter activity. In this study, among four multiple phosphorylation sites in the CTR of AtAMT1;3, we identified the T464 residue in the CTR<sup>C</sup> as inactivating transport activity via ammonium-induced phosphorylation. With the prerequisite of non-phosphorylated T464, a novel T494 residue was uncovered as fine-tuning transporter activity via nitrate-dependent phospho-regulation. These results provide a comprehensive model for how roots regulate nutrient transporter activity via multisite phosphorylation/dephosphorylation in response to various nutrient signals.

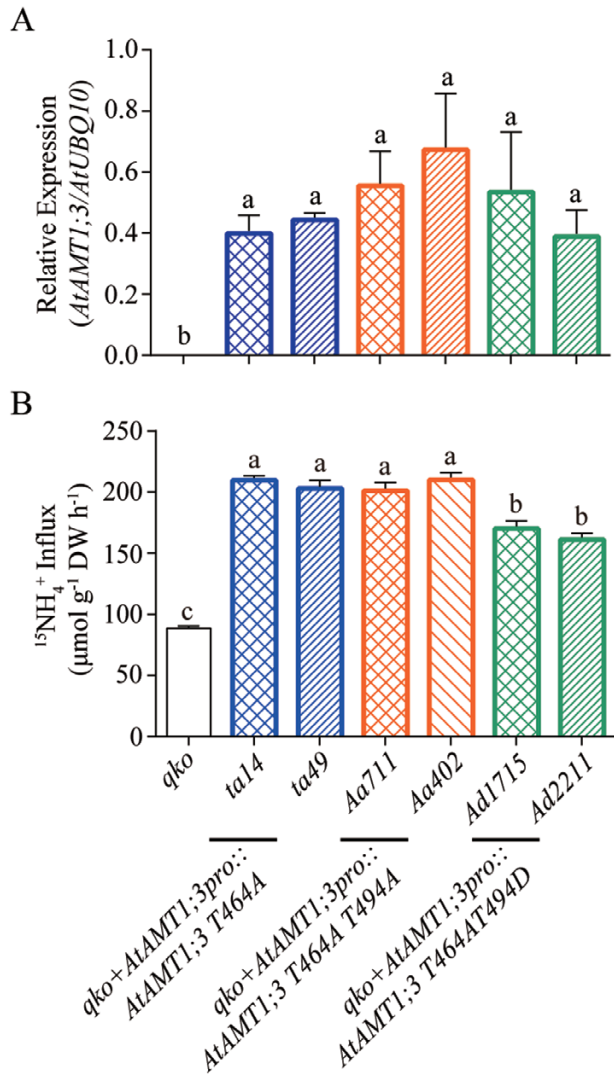


**Fig. 6.** Functional characterization of AtAMT1;3 T464 T494 double phospho-mutants in transgenic Arabidopsis roots. (A) Transcript expression levels of *AtAMT1;3* in roots of *qko*, *qko+AtAMT1;3pro::AtAMT1;3 T464A*, *qko+AtAMT1;3pro::AtAMT1;3 T464A T494A* or *qko+AtAMT1;3pro::AtAMT1;3 T464A T494D* transgenic lines. Levels were quantified by qPCR with three replicates and normalized by *AtUBQ10* expression level. (B) Influx of <sup>15</sup>N-labeled ammonium into roots of the same line as in (A). N-deficient roots were employed for <sup>15</sup>N-labeled ammonium influx assays as determined at the concentration of 250 μM. Bars indicate means ± SD (*n*≥5) and significant differences at *P*<0.001 according to Tukey's test are indicated by different letters. (This figure is available in color at JXB online.)

#### (De-)phosphorylation of T494 in the CTR<sup>NC</sup> fine-tunes AtAMT1;3 transporter activity with dependence on the CTR<sup>C</sup>

The cytosolic C-terminal domain, which is conserved between bacterial, fungal, and plant AMTs, has been demonstrated to serve as an allosteric regulator essential for regulating transport activity, as revealed by X-ray crystal structures and functional mutational analyses *in vitro* or *in vivo* (Loqué et al., 2007; Neuhäuser et al., 2007; Yuan et al., 2013; Boeckstaens et al., 2014; van den Berg et al., 2016). This domain is located in the conserved part of the CTR (CTR<sup>C</sup>) that includes the universally conserved 'ExxGxD' motif (Fig. 2A; Loqué et al.,

2007; van den Berg et al., 2016). With the trimeric complex of AMTs, the interaction between the CTR<sup>C</sup> and cytosolic loops of its own monomer or those of the neighboring monomer controls the opening or closing of the transporters. In plant AMT1s, the CTR<sup>C</sup> undergoes significant conformational changes by phosphorylation of its conserved Thr, thereby breaking its interactions with internal cytosolic loops to inactivate the transporter (Fig. 7; Loqué et al., 2007; Neuhäuser et al., 2007; Yuan et al., 2013).

Several lines of evidence suggest a role of the CTR<sup>NC</sup> in regulating AMT transport activity. First, deletion of the CTR<sup>NC</sup> of AtAMT1;1 (Y469stop; Loqué et al., 2007) and AtAMT1;3 (H474stop; Supplementary Fig. S5) partially reduced their transporter activity. Second, phospho-dependent modifications at T494 located in the CTR<sup>NC</sup> of AtAMT1;3 allowed fine-tuning of transporter activity as shown in yeast, oocytes, and transgenic Arabidopsis roots (Figs 2–4). In addition, the CTR<sup>NC</sup> of the yeast MEP2 was dubbed an auto-inhibitory (AI) region, and deletion of the AI region or phosphorylation of the S457 residue at the AI region is able to activate the transporter function (Boeckstaens et al., 2014; van den Berg et al., 2016). Thus, besides the CTR<sup>C</sup>, the CTR<sup>NC</sup> can be involved in modulating AMT transporter activity, in either a positive or a negative manner.

The structural basis for MEP2 activation by S457 phosphorylation provides a clue for how modification of the CTR<sup>NC</sup> can affect the transporter activity (van den Berg et al., 2016). With S457 phosphorylation at the CTR<sup>NC</sup>, the CTR<sup>C</sup> may undergo a conformational change that is able to establish the interaction of CTR<sup>C</sup> with an inward-moving cytosolic loop for opening the transporter. Although it is unclear whether similar structural arrangements occur in plant AMTs, T494 phosphorylation in the CTR<sup>NC</sup> of AtAMT1;3 is expected to cause conformational changes of the CTR<sup>C</sup>. Unlike that generated by T464 phosphorylation to shut off transport activity completely, this conformational change of the CTR<sup>C</sup> via T494 only moderately reduced transport activity, without changing the affinity for ammonium (Figs 2–4). The CTR<sup>NC</sup> function in modulating AtAMT1;3 transporter activity relies on the CTR<sup>C</sup> as shown by the double phospho-variants in T464 and T494 (Figs 5 and 6; Supplementary Fig. S4). With the non-phospho-mimic T464A, T494 phosphorylation/dephosphorylation modulated function that is probably due to interactions between the CTR<sup>C</sup> and cytosolic loops for fine-tuning transporter activity. The regulatory function of T494, however, is completely lost when phosphorylation mimic T464D disrupts the interaction and closes the transporter.

Multiple phosphorylation sites, at least six Thr/Ser residues, are also present in the C-terminal tail of the Arabidopsis P-type H<sup>+</sup>-ATPase 2 (AHA2) proton pump (Rudashevskaya et al., 2012). Among them, phosphorylation at S899 and S931 decreases the activity, while phosphorylation at T881 or T947 increases the activity (Fuglsang et al., 2007; Takahashi et al., 2012; Haruta et al., 2014; Fuglsang et al., 2014). The phosphorylation at different sites may lead to distinct conformational changes of the C-terminus for these synergistic or antagonistic effects on AtAHA2 activity (Fuglsang et al., 2003). Multisite phosphorylation at the CTR of AtAMT1;3 revealed synergistic effects



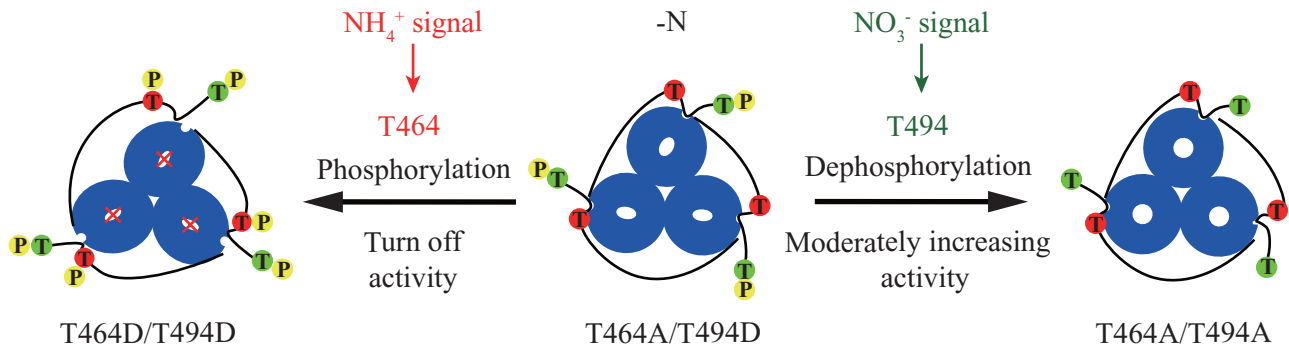


**Fig. 7.** Schematic model for the regulation of AtAMT1;3 transport activity via multisite phosphorylation/dephosphorylation in the C-terminal region. Two phosphorylation sites, T464 (labeled in red) in the CTR<sup>C</sup> and T494 (labeled in green) in the CTR<sup>NC</sup>, are involved in regulating AtAMT1;3 transport activity in response to ammonium and nitrate resupply, respectively. Under N deficiency (-N), AtAMT1;3 is in an active state with T464 non-phosphorylation (without yellow P) and T494 phosphorylation (with yellow P). This is mimicked by the T464A/T494D phospho-variant. Ammonium signals induce T464 phosphorylation (T464D/T494D) for shutting off the transporter activity via the allosteric *trans*-regulatory mechanism preventing excessive uptake of ammonium. Nitrate signals, however, transiently induce ammonium uptake by T494 dephosphorylation (T464A/T494A) for moderate increase of transport activity. Non-phosphorylated T464 is a prerequisite of fine-tuning activity via T494 phosphorylation/dephosphorylation.

on the activities. The phosphorylation/dephosphorylation of T464 at the CTR<sup>C</sup> acted as a prime switch to turn on/off activity, while that of T494 at the CTR<sup>NC</sup> acted as a modulator to fine tune activity, allowing plants to precisely determine ammonium uptake capacity in response to diverse N conditions.

*Multisite (de-)phosphorylation of AtAMT1;3 provides a mechanism for introducing controls of ammonium uptake by different N signaling pathways*

Multisite phosphorylation can occur as phosphorylation at more than one residue by the same protein kinase, or phosphorylation of more than one site by two or more protein kinases (Cohen, 2000). For the latter, multisite phosphorylation is able to modulate the protein function by different kinases/phosphatases via different signaling pathways. To respond to various signals, multiple sites can be phosphorylated with different degrees and even with distinct directions of change for each site, providing a very flexible, but sophisticated, system for precisely regulating protein function (Haruta *et al.*, 2015). For instance, AtAHA2 can be activated by phosphorylation of T947 via the auxin signaling pathway (Takahashi *et al.*, 2012) or by phosphorylation of T881 by the receptor kinase tyrosine-sulfated peptide 1 receptor (PSY1R) via a peptide hormone signal (Fuglsang *et al.*, 2014). This pump can be also inactivated by phosphorylation at other residues, i.e. S899, by receptor-like kinase FER protein kinase (FERONIA) via the peptide rapid alkalization factor (RALF) signal (Haruta *et al.*, 2014) or at S931 by a Ser/Thr kinase PKS5 in response to stress (Fuglsang *et al.*, 2007).

Similar to AtAHA2, the AtAMT1;3 transporter activity can be modulated by multisite phosphorylation under control of different signaling pathways (Figs 1 and 2). The T464 in the CTR<sup>C</sup> is phosphorylated after ammonium signals (Fig. 1). This ammonium-triggered Thr phosphorylation appears highly conserved for all plant AMT1s, i.e. T460 and T472 for AtAMT1;1 and AtAMT1;2, respectively (Straub *et al.*, 2017), T464 for AtAMT1;3 (Fig. 1), and T453 for OsAMT1;2 (Beier *et al.*, 2018). The kinase complex CIPK23-CBL1

phosphorylates AtAMT1;1 and AtAMT1;2, but not AtAMT1;3. Since OsACTPK1, an STY kinase, can phosphorylate the same residue in OsAMT1;2 (Beier *et al.*, 2018), the corresponding Arabidopsis homologs might encode the candidate kinases for phosphorylating AtAMT1;3 at T464. More than one kinase is recruited in ammonium-triggered phosphorylation of conserved Thr in the CTR<sup>C</sup>, ensuring the inhibition of root ammonium uptake under elevated ammonium levels to prevent the risk of ammonium toxicity.

Nitrate signals can induce phosphorylation/dephosphorylation of AtAMT1;3 at several Thr or Ser residues in the CTR<sup>NC</sup> (Fig. 2; Supplementary Fig S2). The direction of phospho-dynamics for each site even differed under nitrate resupply. The T494 residue was transiently dephosphorylated, while S480 and S487 were transiently phosphorylated simultaneously (Fig. 2). The kinetics of changes in T494 phosphorylation status and the associated transporter activity closely paralleled those of ammonium uptake in roots, suggesting a regulatory role of T494 in the nitrate response (Figs 1 and 2). Unexpectedly, phosphorylation-mimicking mutations at either single or double sites of S480 and S487 did not lead to activity changes of AtAMT1;3 mutants in yeast (Fig. 2; Supplementary Fig. S6). The role of phosphorylation at S480 and S487, however, cannot be excluded because their phosphorylation might change subcellular localization, protein degradation, or interaction with other proteins in a plant-specific manner. If so, the yeast system is not suitable to investigate these effects. Nevertheless, mutations at these two residues had no direct effect on transport of ammonium. Unlike a single site phosphorylation control at the CTR<sup>C</sup> dominated by ammonium signals, multisite phosphorylation at CTR<sup>NC</sup> of AMT1s allows introduction of control by diverse N-related signaling pathways (i.e. nitrate, light, and hormone signals) (Supplementary Table S2). Indeed, multisite phosphorylation is required in the root epidermis-expressed AtAMT1;1 and AtAMT1;3, which allows precise regulation of the symplastic ammonium transport in response to multiple signals in dynamic environments. For the endodermis-expressed AtAMT1;2 that mediates the apoplastic transport pathway, by contrast, the presence of a single Thr<sup>CTR</sup>

phosphorylation may be sufficient to shut off transport activity under high external ammonium, preventing excessive ammonium allocation to the more sensitive shoot.

Taken together, our data present a model for (de-) phosphorylation-based regulation of AtAMT1;3 at multiple phosphorylation sites under control of different N signals, which may be conserved in other plant AMT1s (Fig. 7). In N-deficient roots, AtAMT1;3 is present in an active form with non-phosphorylated T464 in the CTR<sup>C</sup> and phosphorylated T494 in the CTR<sup>NC</sup> (mimicked by T464A T494D). Ammonium signals rapidly induce T464 phosphorylation (T464D T494D) to shut off transport activity, preventing excessive uptake of ammonium. Nitrate signals, on the contrary, transiently induce ammonium uptake by T494 dephosphorylation (T464A T494A). This allows elevation of the activity of AtAMT1;3, which transports NH<sub>4</sub><sup>+</sup> as a counter ion to nitrate. The uptake is returned to the original level after T494 re-phosphorylation. Considering that ammonium and nitrate are a major cation and anion, respectively, in plants, the nitrate-triggered transient induction of ammonium uptake is probably relevant to change the uptake balance of both ions (Kronzucker *et al.*, 1999; Babourina *et al.*, 2007; Luo *et al.*, 2013; Hachiya and Sakakibara, 2017). The CIPK23–CBL1 kinase complex is supposed to sense ammonium, nitrate, and potassium simultaneously for controlling cellular ion homeostasis (Xu *et al.*, 2006; Ho *et al.*, 2009; Straub *et al.*, 2017). Given that many kinases and phosphatases are regulated via the nitrate signaling pathway (Undurraga *et al.*, 2017), identification of those upstream modulators of AMT1s will be of great interest for further research.

## Supplementary data

Supplementary data are available at *JXB* online.

Fig. S1. Transcript expression levels of *AtAMT1;3* in *qko+13* roots in response to ammonium and nitrate resupply.

Fig. S2. Phosphorylation dynamics of *AtAMT1;3* CTR<sup>NC</sup> at multiple sites (S480, S487, and T494) in response to nitrate or ammonium.

Fig. S3. Yeast growth complementation of *AtAMT1;3* S480, S487, and T494 single phospho-mutants.

Fig. S4. Functional characterization of *AtAMT1;3* T494 single phospho-mutants and T464 T494 double phospho-mutants in *Xenopus* oocytes.

Fig. S5. Yeast growth complementation of *AtAMT1;3* CTR<sup>NC</sup> deletion mutant.

Fig. S6. Functional characterization of *AtAMT1;3* T464 S480 S487 triple phospho-mutants in yeast.

Table S1. Primers used in this study.

Table S2. *In vivo* phosphorylation sites in the C-terminal region of *AtAMT1s*.

## Acknowledgements

We thank the anonymous reviewers for their critical readings and constructive comments on the manuscript.

## Funding

This work was financially supported by the National Natural Science Foundation of China (NSFC) [31430095; 31471934; 30971863; 30870189], and the Deutsche Forschungsgemeinschaft (DFG) [328017493/GRK 2366].

## Author contributions

XW and LY conceived and designed the research. XW, TL, YZ, FD, and BN performed the experiments. XW, BN, UL, WS, and LY analysed the data. XW and LY wrote the manuscript and BN, UL, and WS helped to revise the manuscript. All authors read and approved the manuscript. The authors declare no conflict of interest.

## References

- Babourina O, Voltchanskii K, McGann B, Newman I, Rengel Z. 2007. Nitrate supply affects ammonium transport in canola roots. *Journal of Experimental Botany* **58**, 651–658.
- Baukowitz T, Tucker SJ, Schulte U, Benndorf K, Ruppersberg JP, Fakler B. 1999. Inward rectification in K<sub>ATP</sub> channels: a pH switch in the pore. *The EMBO Journal* **18**, 847–853.
- Bayle V, Arrighi JF, Creff A, Nespoulous C, Vialaret J, Rossignol M, Gonzalez E, Paz-Ares J, Nussaume L. 2011. *Arabidopsis thaliana* high-affinity phosphate transporters exhibit multiple levels of posttranslational regulation. *The Plant Cell* **23**, 1523–1535.
- Beier MP, Obara M, Tanai A, *et al.* 2018. Lack of ACTPK1, an STY kinase, enhances ammonium uptake and use, and promotes growth of rice seedlings under sufficient external ammonium. *The Plant Journal* **93**, 992–1006.
- Boeckstaens M, Linares E, Van Vooren P, Marini AM. 2014. The TORC1 effector kinase Npr1 fine tunes the inherent activity of the Mep2 ammonium transport protein. *Nature Communications* **5**, 3101.
- Boudsocq M, Willmann MR, McCormack M, Lee H, Shan L, He P, Bush J, Cheng SH, Sheen J. 2010. Differential innate immune signalling via Ca<sup>2+</sup> sensor protein kinases. *Nature* **464**, 418–422.
- Clough SJ, Bent AF. 1998. Floral dip: a simplified method for *Agrobacterium*-mediated transformation of *Arabidopsis thaliana*. *The Plant Journal* **16**, 735–743.
- Cohen P. 2000. The regulation of protein function by multisite phosphorylation – a 25 year update. *Trends in Biochemical Sciences* **25**, 596–601.
- Duan F, Giehl RFH, Geldner N, Salt DE, von Wirén N. 2018. Root zone-specific localization of AMTs determines ammonium transport pathways and nitrogen allocation to shoots. *PLoS Biology* **16**, e2006024.
- Engelsberger WR, Schulze WX. 2012. Nitrate and ammonium lead to distinct global dynamic phosphorylation patterns when resupplied to nitrogen-starved *Arabidopsis* seedlings. *The Plant Journal* **69**, 978–995.
- Fuglsang AT, Borch J, Bych K, Jahn TP, Roepstorff P, Palmgren MG. 2003. The binding site for regulatory 14-3-3 protein in plant plasma membrane H<sup>+</sup>-ATPase involves a region promoting phosphorylation-independent interaction in addition to the phosphorylation-dependent C-terminal end. *The Journal of Biological Chemistry* **278**, 42266–42272.
- Fuglsang AT, Guo Y, Cuin TA, *et al.* 2007. *Arabidopsis* protein kinase PKS5 inhibits the plasma membrane H<sup>+</sup>-ATPase by preventing interaction with 14-3-3 protein. *The Plant Cell* **19**, 1617–1634.
- Fuglsang AT, Kristensen A, Cuin TA, *et al.* 2014. Receptor kinase-mediated control of primary active proton pumping at the plasma membrane. *The Plant Journal* **80**, 951–964.
- Gazzarrini S, Lejay L, Gojon A, Ninnemann O, Frommer WB, von Wirén N. 1999. Three functional transporters for constitutive, diurnally regulated, and starvation-induced uptake of ammonium into *Arabidopsis* roots. *The Plant Cell* **11**, 937–948.
- Giehl RFH, Laginha AM, Duan F, Rentsch D, Yuan L, von Wirén N. 2017. A critical role of AMT2;1 in root-to-shoot translocation of ammonium in *Arabidopsis*. *Molecular Plant* **10**, 1449–1460.

- Gu R, Duan F, An X, Zhang F, von Wirén N, Yuan L.** 2013. Characterization of AMT-mediated high-affinity ammonium uptake in roots of maize (*Zea mays* L.). *Plant & Cell Physiology* **54**, 1515–1524.
- Hachiya T, Sakakibara H.** 2017. Interactions between nitrate and ammonium in their uptake, allocation, assimilation, and signaling in plants. *Journal of Experimental Botany* **68**, 2501–2512.
- Haruta M, Gray WM, Sussman MR.** 2015. Regulation of the plasma membrane proton pump ( $H^+$ -ATPase) by phosphorylation. *Current Opinion in Plant Biology* **28**, 68–75.
- Haruta M, Sabat G, Stecker K, Minkoff BB, Sussman MR.** 2014. A peptide hormone and its receptor protein kinase regulate plant cell expansion. *Science* **343**, 408–411.
- Ho CH, Lin SH, Hu HC, Tsay YF.** 2009. CHL1 functions as a nitrate sensor in plants. *Cell* **138**, 1184–1194.
- Kaiser BN, Rawat SR, Siddiqi MY, Masle J, Glass AD.** 2002. Functional analysis of an Arabidopsis T-DNA “knockout” of the high-affinity  $NH_4^+$  transporter AtAMT1;1. *Plant Physiology* **130**, 1263–1275.
- Khademi S, O’Connell J 3rd, Remis J, Robles-Colmenares Y, Miercke LJ, Stroud RM.** 2004. Mechanism of ammonia transport by Amt/MEP/Rh: structure of AmtB at 1.35 Å. *Science* **305**, 1587–1594.
- Kiba T, Inaba J, Kudo T, et al.** 2018. Repression of nitrogen starvation responses by members of the Arabidopsis GARP-type transcription factor NIGT1/HRS1 subfamily. *The Plant Cell* **30**, 925–945.
- Kronzucker HJ, Siddiqi MY, Glass AD, Kirk GJ.** 1999. Nitrate-ammonium synergism in rice. A subcellular flux analysis. *Plant Physiology* **119**, 1041–1046.
- Lanquar V, Loqué D, Hörmann F, Yuan L, Bohner A, Engelsberger WR, Lalonde S, Schulze WX, von Wirén N, Frommer WB.** 2009. Feedback inhibition of ammonium uptake by a phospho-dependent allosteric mechanism in *Arabidopsis*. *The Plant Cell* **21**, 3610–3622.
- Li S, Tian Y, Wu K, et al.** 2018. Modulating plant growth-metabolism coordination for sustainable agriculture. *Nature* **560**, 595–600.
- Lima JE, Kojima S, Takahashi H, von Wirén N.** 2010. Ammonium triggers lateral root branching in *Arabidopsis* in an AMMONIUM TRANSPORTER1;3-dependent manner. *The Plant Cell* **22**, 3621–3633.
- Liu Y, von Wirén N.** 2017. Ammonium as a signal for physiological and morphological responses in plants. *Journal of Experimental Botany* **68**, 2581–2592.
- Loqué D, Lalonde S, Looger LL, von Wirén N, Frommer WB.** 2007. A cytosolic *trans*-activation domain essential for ammonium uptake. *Nature* **446**, 195–198.
- Loqué D, Mora SI, Andrade SL, Pantoja O, Frommer WB.** 2009. Pore mutations in ammonium transporter AMT1 with increased electrogenic ammonium transport activity. *The Journal of Biological Chemistry* **284**, 24988–24995.
- Loqué D, von Wirén N.** 2004. Regulatory levels for the transport of ammonium in plant roots. *Journal of Experimental Botany* **55**, 1293–1305.
- Loqué D, Yuan L, Kojima S, Gojon A, Wirth J, Gazzarrini S, Ishiyama K, Takahashi H, von Wirén N.** 2006. Additive contribution of AMT1;1 and AMT1;3 to high-affinity ammonium uptake across the plasma membrane of nitrogen-deficient *Arabidopsis* roots. *The Plant Journal* **48**, 522–534.
- Luo J, Qin J, He F, Li H, Liu T, Polle A, Peng C, Luo ZB.** 2013. Net fluxes of ammonium and nitrate in association with  $H^+$  fluxes in fine roots of *Populus popularis*. *Planta* **237**, 919–931.
- Marini AM, Soussi-Boudekou S, Vissers S, Andre B.** 1997. A family of ammonium transporters in *Saccharomyces cerevisiae*. *Molecular and Cellular Biology* **17**, 4282–4293.
- Marschner P, Rengel Z.** 2012. Nutrient availability in soils. In: Marschner P, ed. *Marschner’s mineral nutrition of higher plants*, 3rd edn. San Diego: Academic Press, 315–330.
- Mayer M, Dynowski M, Ludewig U.** 2006. Ammonium ion transport by the AMT/Rh homologue LeAMT1;1. *The Biochemical Journal* **396**, 431–437.
- Mayer M, Ludewig U.** 2006. Role of AMT1;1 in  $NH_4^+$  acquisition in *Arabidopsis thaliana*. *Plant Biology* **8**, 522–528.
- Menz J, Li Z, Schulze WX, Ludewig U.** 2016. Early nitrogen-deprivation responses in *Arabidopsis* roots reveal distinct differences on transcriptome and (phospho-) proteome levels between nitrate and ammonium nutrition. *The Plant Journal* **88**, 717–734.
- Neuhäuser B, Dynowski M, Ludewig U.** 2009. Channel-like  $NH_3$  flux by ammonium transporter AtAMT2. *FEBS Letters* **583**, 2833–2838.
- Neuhäuser B, Dynowski M, Mayer M, Ludewig U.** 2007. Regulation of  $NH_4^+$  transport by essential cross talk between AMT monomers through the carboxyl tails. *Plant Physiology* **143**, 1651–1659.
- Rawat SR, Silim SN, Kronzucker HJ, Siddiqi MY, Glass AD.** 1999. AtAMT1 gene expression and  $NH_4^+$  uptake in roots of *Arabidopsis thaliana*: evidence for regulation by root glutamine levels. *The Plant Journal* **19**, 143–152.
- Rudashevskaya EL, Ye J, Jensen ON, Fuglsang AT, Palmgren MG.** 2012. Phosphosite mapping of P-type plasma membrane  $H^+$ -ATPase in homologous and heterologous environments. *The Journal of Biological Chemistry* **287**, 4904–4913.
- Sonoda Y, Ikeda A, Saiki S, von Wirén N, Yamaya T, Yamaguchi J.** 2003a. Distinct expression and function of three ammonium transporter genes (*OsAMT1;1–1;3*) in rice. *Plant & Cell Physiology* **44**, 726–734.
- Sonoda Y, Ikeda A, Saiki S, Yamaya T, Yamaguchi J.** 2003b. Feedback regulation of the ammonium transporter gene family *AMT1* by glutamine in rice. *Plant & Cell Physiology* **44**, 1396–1402.
- Straub T, Ludewig U, Neuhäuser B.** 2017. The kinase CIPK23 inhibits ammonium transport in *Arabidopsis thaliana*. *The Plant Cell* **29**, 409–422.
- Takahashi K, Hayashi K, Kinoshita T.** 2012. Auxin activates the plasma membrane  $H^+$ -ATPase by phosphorylation during hypocotyl elongation in *Arabidopsis*. *Plant Physiology* **159**, 632–641.
- Undurraga SF, Ibarra-Henríquez C, Fredes I, Álvarez JM, Gutiérrez RA.** 2017. Nitrate signaling and early responses in *Arabidopsis* roots. *Journal of Experimental Botany* **68**, 2541–2551.
- van den Berg B, Chembath A, Jefferies D, Basle A, Khalid S, Rutherford JC.** 2016. Structural basis for Mep2 ammonium transporter activation by phosphorylation. *Nature Communications* **7**, 11337.
- von Wirén N, Gazzarrini S, Gojon A, Frommer WB.** 2000. The molecular physiology of ammonium uptake and retrieval. *Current Opinion in Plant Biology* **3**, 254–261.
- Wu X, Yang H, Qu C, Xu Z, Li W, Hao B, Yang C, Sun G, Liu G.** 2015. Sequence and expression analysis of the AMT gene family in poplar. *Frontiers in Plant Science* **6**, 337.
- Xu J, Li HD, Chen LQ, Wang Y, Liu LL, He L, Wu WH.** 2006. A protein kinase, interacting with two calcineurin B-like proteins, regulates  $K^+$  transporter AKT1 in *Arabidopsis*. *Cell* **125**, 1347–1360.
- Xuan YH, Priatama RA, Huang J, et al.** 2013. Indeterminate domain 10 regulates ammonium-mediated gene expression in rice roots. *New Phytologist* **197**, 791–804.
- Yuan L, Gu R, Xuan Y, Smith-Valle E, Loqué D, Frommer WB, von Wirén N.** 2013. Allosteric regulation of transport activity by heterotrimerization of *Arabidopsis* ammonium transporter complexes in vivo. *The Plant Cell* **25**, 974–984.
- Yuan L, Loqué D, Kojima S, Rauch S, Ishiyama K, Inoue E, Takahashi H, von Wirén N.** 2007a. The organization of high-affinity ammonium uptake in *Arabidopsis* roots depends on the spatial arrangement and biochemical properties of AMT1-type transporters. *The Plant Cell* **19**, 2636–2652.
- Yuan L, Loqué D, Ye F, Frommer WB, von Wirén N.** 2007b. Nitrogen-dependent posttranscriptional regulation of the ammonium transporter AtAMT1;1. *Plant Physiology* **143**, 732–744.